Check for updates

JGR Biogeosciences

RESEARCH ARTICLE
10.1029/2023JG007620

Legacy Phosphorus and Ecosystem Memory Control Future Water Quality in a Eutrophic Lake

P. C. Hanson[1], R. Ladwig[1], C. Buelo[1], E. A. Albright[1], A. D. Delany[1], and C. C. Carey[2]

[1]Center for Limnology, University of Wisconsin-Madison, Madison, WI, USA, [2]Department of Biological Sciences, Virginia Tech, Blacksburg, VA, USA

Key Points:

- Legacy phosphorus in lake sediments controls long term lake water quality response to nutrient remediation
- Coupled cycles of nutrients, physics, and metabolism explain ecosystem memory of lake phosphorus, water clarity, and oxygen habitat
- Improvement in lake water quality to pristine levels will require decades of commitment to nutrient load reductions

Supporting Information:

Supporting Information may be found in the online version of this article.

Correspondence to:

P. C. Hanson,
pchanson@wisc.edu

Citation:

Hanson, P. C., Ladwig, R., Buelo, C., Albright, E. A., Delany, A. D., & Carey, C. C. (2023). Legacy phosphorus and ecosystem memory control future water quality in a eutrophic lake. *Journal of Geophysical Research: Biogeosciences*, *128*, e2023JG007620. https://doi.org/10.1029/2023JG007620

Received 10 JUN 2023
Accepted 9 NOV 2023

Abstract Lake water clarity, phytoplankton biomass, and hypolimnetic oxygen concentration are metrics of water quality that are highly degraded in eutrophic systems. Eutrophication is linked to legacy nutrients stored in catchment soils and in lake sediments. Long lags in water quality improvement under scenarios of nutrient load reduction to lakes indicate an apparent ecosystem memory tied to the interactions between water biogeochemistry and lake sediment nutrients. To investigate how nutrient legacies and ecosystem memory control lake water quality dynamics, we coupled nutrient cycling and lake metabolism in a model to recreate long-term water quality of a eutrophic lake (Lake Mendota, Wisconsin, USA). We modeled long-term recovery of water quality under scenarios of nutrient load reduction and found that the rates and patterns of water quality improvement depended on changes in phosphorus (P) and organic carbon storage in the water column and sediments. Through scenarios of water quality improvement, we showed that water quality variables have distinct phases of change determined by the turnover rates of storage pools—an initial and rapid water quality improvement due to water column flushing, followed by a much longer and slower improvement as sediment P pools were slowly reduced. Water clarity, phytoplankton biomass, and hypolimnetic dissolved oxygen differed in their time responses. Water clarity and algal biomass improved within years of nutrient reductions, but hypolimnetic oxygen took decades to improve. Even with reduced catchment loading, recovery of Lake Mendota to a mesotrophic state may require decades due to nutrient legacies and long ecosystem memory.

Plain Language Summary Lake water quality, as measured by algae concentration near the lake surface, the clarity of the water, and the availability of dissolved oxygen, is greatly reduced in lakes with nutrient pollution from phosphorus. In Lake Mendota, Wisconsin, phosphorus applied to the surrounding landscape for more than a century has accumulated in catchment soils and in the lake water column and sediments (i.e., "legacy phosphorus"), leading to poor water quality. To investigate how water quality in Lake Mendota might respond to nutrient reduction, we used computer models to simulate the elimination of phosphorus inputs from the catchment and track water quality change. Phosphorus in the lake water column initially decreased quickly, due to water column flushing, but then decreased very slowly due to release of legacy phosphorus from lake sediments. Water quality recovery lagged that of phosphorus, indicating an inherent "ecosystem memory" for past phosphorus levels. Ecosystem memory was due to biological activity that remained elevated, even when phosphorus was declining in the water column. When nutrient inputs to the lake were eliminated in the model, recovery of algae concentrations and water clarity to pristine conditions required decades, and a return to a fully oxygenated condition required a century.

1. Introduction

The quality of surface freshwater underpins sustainable futures for the planet (Folke et al., 2020; Lee & Diop, 2009); however, water quality deterioration has been alarmingly persistent (Damania et al., 2019; Oliver et al., 2017). Human activities have greatly exacerbated lake eutrophication, or excess nutrient enrichment, which drives toxic phytoplankton blooms, reduced water clarity, and bottom water anoxia (Smith & Schindler, 2009). Eutrophication is associated with heightened nutrient loads to lakes (Schindler et al., 2016), especially watershed nitrogen (N) and phosphorus (P) export from lake catchments (Carpenter & Bennett, 2011). Water quality in lakes has shown troubling resistance to improvement, despite recognition of the problem and management action intended to reduce nutrient loads (Jenny et al., 2016; Søndergaard et al., 2007).

Slow recovery of lake water quality is due, in part, to the legacy of nutrient application in lake catchments (Chen et al., 2018). Here, we refer to nutrient legacies following Van Meter et al. (2018), specifically referring

© 2023 The Authors.
This is an open access article under the terms of the Creative Commons Attribution-NonCommercial License, which permits use, distribution and reproduction in any medium, provided the original work is properly cited and is not used for commercial purposes.

21698961, 2023, 12, Downloaded from https://agupubs.onlinelibrary.wiley.com/doi/10.1029/2023JG007620, Wiley Online Library on [12/12/2023]. See the Terms and Conditions (https://onlinelibrary.wiley.com/terms-and-conditions) on Wiley Online Library for rules of use; OA articles are governed by the applicable Creative Commons License

to the excess N and P accumulated in catchment terrestrial soils due to decades of agriculture and other land use (Bennett et al., 1999; Sabo et al., 2021). For many catchments, the effect of this nutrient legacy is eutrophication in downstream lake ecosystems (Bennett et al., 1999; Keatley et al., 2011; Van Meter et al., 2021). Although catchment-scale nutrient management programs have led to reduced nutrient export to lakes in some cases (Sharpley et al., 2019), lakes can be slow to recover from eutrophication (McCrackin et al., 2017), due in part to legacy nutrients accumulated in lake sediments (Faridmarandi et al., 2020; Jeppesen et al., 2005).

Ecosystem memory in lakes may contribute to slow recovery from eutrophication. Here, we define ecosystem memory (sensu, Ogle et al., 2015) as the influence of past ecosystem states on the rates and patterns of future responses to change. In lakes, many processes may contribute to ecosystem memory and associated responses to nutrient load reductions, such as slow flushing in lakes with long hydrologic residence times (Hotchkiss et al., 2018), internal loading of nutrients from large sediment pools (Carleton & Lee, 2023; Missimer et al., 2020; Søndergaard et al., 2007), and biological feedback mechanisms that promote persistently high algal biomass, despite decreasing nutrient loads (Scheffer et al., 2001). While specific biophysical processes may be well described, it remains a challenge to understand how their interactions control water quality metrics that emerge at the ecosystem scale, such as seasonal patterns of phytoplankton biomass, water clarity, and formation of deep-water anoxia.

Lake metabolism provides a framework for investigating ecosystem memory by linking changes in nutrient concentration to biophysical processes that can be expressed as ecosystem-scale water quality metrics over different time scales. While lake metabolism can be generalized as the balance of primary production and respiration (Odum, 1956; Staehr et al., 2010), its implementation in analytical models often includes physical and biological processes that quantify both metabolic processes and ecosystem states relevant to water quality (Ladwig et al., 2022; Winslow et al., 2016). For example, elevated epilimnetic nutrients stimulate primary production (i.e., autochthony), which reduces water clarity through phytoplankton-associated turbidity (Smith, 1982). Autochthonous organic matter supports high microbial respiration, which leads to consumption of available oxygen in deeper waters of thermally stratified lakes (Matzinger et al., 2010; Müller et al., 2012). Allochthonous organic matter also contributes to lake metabolism (Hanson et al., 2003) and is generally considered a more recalcitrant and persistent source of organic carbon that contributes to long-term change in water quality metrics (Kothawala et al., 2014). Metabolism models that consider both autochthonous and allochthonous organic matter sources and cycling can recreate both short-term and long-term ecosystem dynamics (Hoellein et al., 2013). By linking physical, nutrient, and organic carbon cycles, metabolism models may also provide a mechanistic basis for the role of ecosystem memory in eutrophication recovery.

We investigated how linked cycles of phosphorus (P), carbon (C), and lake metabolism control the time scale of water quality responses to reduced nutrient loads projected for Lake Mendota (Wisconsin, USA). We used 20 years of observational data to calibrate a physical-biogeochemical model and recreate annual dynamics of three water quality metrics, which are water column P concentrations, water clarity (as a function of dissolved and particulate organic carbon), and hypolimnetic dissolved oxygen (DO) depletion. Through a scenario of long-term nutrient reduction, we quantified how P legacies in the lake influence the responses of water quality metrics, highlighting the role of long-term ecosystem memory. While we were interested in water quality recovery, we were equally interested in the internal feedbacks that alter the time scales of change for water quality to address the questions: How do P cycles and lake metabolism interact to determine the time scales of change for water clarity and summer anoxia? How long is the legacy of historical P loading from the catchment to the lake on future water quality conditions?

2. Materials and Methods

Our overarching modeling strategy was to link sediment and water column nutrient and organic matter cycles for the purpose of investigating how seasonal water quality metrics change over decades to centuries. While there are excellent examples of coupling sediment to water processes (reviewed by Paraska et al., 2014), we needed an approach that allowed us to model lake metabolism at the ecosystem scale and that included general sediment properties, such as area, depth and P and organic carbon (OC) pool sizes. Following the recent work by Carleton and Lee (2023), who used a relatively simple model to recreate long-term P change in lakes and their sediments, we focus on simplicity and flexibility, recognizing that our approach enables future scaling to build additional complexity and application. We also placed high importance on recreating both seasonal and long-term dynamics

21698961, 2023, 12, Downloaded from https://agupubs.onlinelibrary.wiley.com/doi/10.1029/2023JG007620, Wiley Online Library on [12/12/2023]. See the Terms and Conditions (https://onlinelibrary.wiley.com/terms-and-conditions) on Wiley Online Library for rules of use; OA articles are governed by the applicable Creative Commons License

in addressing how a lake responds to nutrient load reduction. Seasonal dynamics are important because water quality impairment, such as algal blooms and hypolimnetic anoxia, are generally summer phenomena in north temperate lakes. Long-term dynamics (decades to centuries) are important because of the persistence of nutrient legacies in lakes. We relied on high quality long-term data to inform the design of the model and calibrated it for predicting water quality. We used the calibrated model to run scenarios of water quality recovery, in which external nutrient loads to the lake were reduced.

2.1. Study System

Our study system was Lake Mendota, which is a eutrophic lake located in south-central Wisconsin, USA. The lake's surface area is 39.61 km^2, with a maximum and mean depth of 25 and 12.8 m, respectively. The lake has a dimictic mixing regime and typically is stratified during most of April-October. Lake Mendota is a drainage lake with an average water residence time of 4.3 years (Lathrop & Carpenter, 2014).

Lake Mendota and its catchment have a long history of human use. While people have lived near Lake Mendota for thousands of years, eutrophication likely occurred over a relatively short time period during the late 1800s to early 1900s, due to agricultural intensification, followed by urbanization (Brock, 1985; Lathrop, 2007). For our study, we assumed that Lake Mendota was either mesotrophic or oligotrophic in its water quality prior to European settlement, based on sediment cores (Brock, 1985). Currently, the lake is eutrophic and its catchment is predominantly urban and agricultural, with very high N and P mass in catchment soils (Bennett et al., 1999; Lathrop, 2007). As a result of decades of high N export from the catchment to the lake, the lake tends to be P-limited (Lathrop, 2007), and thus we focused on P dynamics when modeling the nutrient legacies of the lake.

2.2. Models Linking Physics, Phosphorus, Organic Carbon, and Dissolved Oxygen

We used a time-dynamic approach to model lake water quality and linked the three lake water quality cycles of interest—P, OC, and DO, all within the context of lake hydrodynamics (Figure 1). We used this model to generate daily metrics of water quality, which are water column P concentrations, water clarity (as a function of dissolved and particulate OC), and hypolimnetic DO depletion. To study long-term changes in water quality, we tracked ecosystem states in both the water column and sediments. Explicitly linking cycles of P, OC, and DO enabled us to study how changes in external loads led to changes in major lake pools and subsequent changes in seasonal water quality metrics.

Model details are provided in Supporting Information S1 (Tables S1–S3). The process-based implementation of thermodynamics was adapted from our previous work on pond thermal structure (Albright et al., 2022), lake metabolism modeling (Carey et al., 2018), and lake phosphorus modeling (Hanson et al., 2020). The model is 1-D in the vertical dimension, with three compartments modeled simultaneously using a box-modeling approach—water column epilimnion and hypolimnion, and active sediments (Figure 1). Each compartment is treated as fully mixed.

The lake physical model solves the energy budget and mixing dynamics on an hourly time step and produces 1 m vertical resolution temperature output. The lake physical model follows an integral energy approach for heat transport and solves vertical diffusion using an implicit scheme (see model formulations in Albright et al., 2022; note that we neglected the effects of macrophytes on energy attenuation in the current study). Water clarity, updated daily by the metabolism model, informs attenuation of short-wave radiation in the physical model. Hourly temperature output by the physical model is averaged to daily values, and sequentially linked to the water quality calculations. Thermal strata are calculated from the vertical temperature gradient. Strata volume and areal contact with sediments are calculated daily from the thermocline depth and lake hypsometry. In our application of the physical model output in the metabolism model, each thermal layer was considered fully mixed, and mean layer temperature was calculated from the layer's volume weighted average.

The metabolism model includes pools (i.e., state variables) of total phosphorus (P), organic carbon (OC), and dissolved oxygen (DO) (Figure 1; Table S1 in Supporting Information S1). OC pools include particulate (POC) and dissolved (DOC) fractions with labile (POC_L, DOC_L) and recalcitrant (POC_R, DOC_R) forms. The model information is provided in detail in Supporting Information S1, and summarized here. Pools are tracked separately for the epilimnion and the hypolimnion. We assume allochthony is recalcitrant and autochthony is labile.

21698961, 2023, 12, Downloaded from https://agupubs.onlinelibrary.wiley.com/doi/10.1029/2023JG007620, Wiley Online Library on [12/12/2023]. See the Terms and Conditions (https://onlinelibrary.wiley.com/terms-and-conditions) on Wiley Online Library for rules of use; OA articles are governed by the applicable Creative Commons License

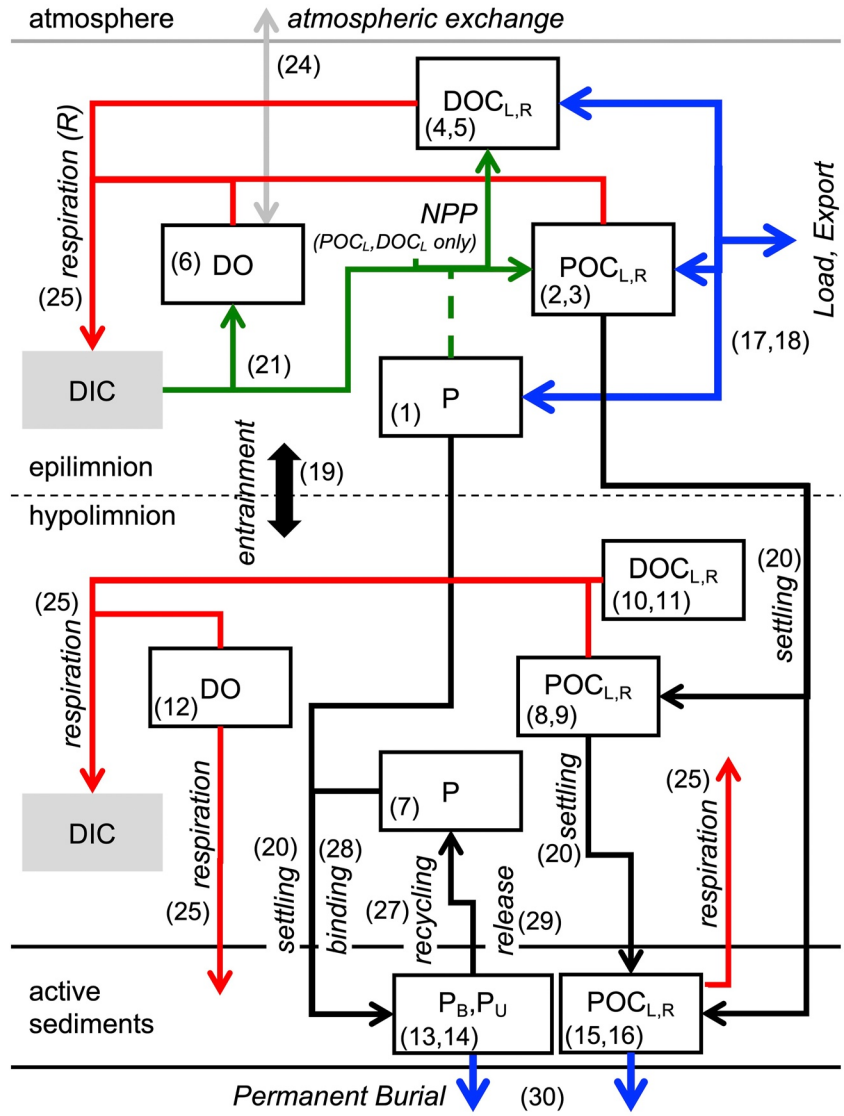

Figure 1. The lake model has three compartments: epilimnion, hypolimnion (when the lake is thermally stratified), and active sediments. Boxes are state variables. DIC shown for reference and is not modeled. Arrows are fluxes or biogeochemical transformations. Modeled state variables are: phosphorus (P); in the sediments, P is divided between bound (P_B) and unbound (P_U) forms; dissolved oxygen (DO); particulate and dissolved organic carbon (POC and DOC, respectively) in two forms, labile (*OC_L) and recalcitrant (*OC_R). Three fluxes control ecosystem inputs and outputs for P and OC (blue arrows)—load, export, and burial. Movement of state variables between compartments indicated by black arrows. Metabolic processes are net primary production (NPP) (green) and respiration (R) (red). The dashed green arrow indicates that NPP is not a sink for P in our model and that P does not become part of the DOC pool. P efflux from the sediments is represented as recycling of P_U and release of P_B. Settling and rebinding return P to the sediments. All state variables are subject to entrainment as the thermocline depth changes. Numbers in parentheses refer to model equations (Table S1 in Supporting Information S1).

The model also includes an "active sediment layer," which has pools for labile and recalcitrant POC and pools for tightly bound P (P_B) and loosely bound (including organic) P, which we simplified to "unbound" (P_U). At a conceptual level, our overall approach has similarities that of Carleton and Lee (2023) on P cycling in lakes. We highlight in Supporting Information S1 some key similarities and differences between their work and ours, and we use the findings of Carleton and Lee (2023) and references therein in evaluating the long-term behavior of our model.

The lake sediments are divided into an active sediment layer above a permanent burial zone. The active zone has POC_R, POC_L, P_U, and P_B, each of which interacts with the water column and is subject to permanent burial.

21698961, 2023, 12, Downloaded from https://agupubs.onlinelibrary.wiley.com/doi/10.1029/2023JG007620, Wiley Online Library on [12/12/2023]. See the Terms and Conditions (https://onlinelibrary.wiley.com/terms-and-conditions) on Wiley Online Library for rules of use; OA articles are governed by the applicable Creative Commons License

Sources of sediment $POC_{R,L}$ are settling from the water column. Sinks for $POC_{R,L}$ include mineralization to inorganic carbon and permanent burial. Sources for sediment P are settling (P_U) and rebinding (P_B) from the water column. Sinks for $P_{U,B}$ include recycling of P_U back into the water column, release of P_B back into the water column under anoxic conditions, and permanent burial of $P_{U,B}$. The details of rates and how they vary by temperature and oxic condition are provided in Supporting Information S1. Permanent burial of P and OC is determined by the accumulation of lake sediments. A sediment accumulation rate of 1.0 mm y^{-1} is assumed for Lake Mendota, unless otherwise stated in a scenario. While roughly half of the accumulation rate found previously for Lake Mendota sediment cores (Lathrop, 2007; Walsh et al., 2019), we used a lower rate due to sediment focusing not accounted in previous estimates. Permanent burial of P and OC is simply the product of the mass of each of the active sediment constituents and the ratio of the sedimentation rate and active sediment depth. For example, under the above conditions, permanent burial of POC would be $POC_{Sed} \times 0.001$ m $y^{-1}/0.1$ m $= POC_{Sed} \times 0.01$ $years^{-1}$. We explore some of these assumptions in scenarios described below. See Supporting Information S1 for more detailed justification for sediment extent and dynamics.

2.3. Model Calibration and Sensitivity Analysis

The model was manually calibrated to recreate observed ice cover onset and breakup, Secchi depth, and volumetrically-weighted mean values for the epilimnion and hypolimnion for water temperature, dissolved oxygen, total phosphorus, and dissolved organic carbon. To compare model output to Secchi depth, we calculated a light extinction coefficient for the water column as a function of the dissolved and particulate OC output from the model, and converted light extinction coefficient to Secchi depth (Equation S23 in Supporting Information S1). Calibration was based on the ~20 years of observational data from 1995 to 2015. Free parameters (Table S2 in Supporting Information S1) were manually tuned to achieve visual correspondence between predictions and observations. Root mean square error (RMSE), Nash–Sutcliffe model efficiency coefficient (NSE), and Kling-Gupta Efficiency (KGE) are reported for the fit model over the calibration period.

We assumed that the calibrated model must approximate sediment core values of P. As described previously, it was necessary to run the model for hundreds of years (repeating the 20 years of driving data) to achieve sediment equilibrium for both P and OC. Because P recycling and sediment respiration are a function of sediment P and OC pool sizes, a change in equilibrium of the sediments affects water column predictions, requiring additional calibration. Thus, calibration was an iterative process of selecting parameter values, running the model for centuries to long-term equilibrium, and then checking for calibration. Although automated optimization would likely yield more accurate predictions, the dominant sensitivities lie more in our assumptions regarding P pools and loads.

For the legacy scenarios described below, we did not have observational data for the Lake Mendota prior to western settlement. To test whether our calibrated model could reproduce oligotrophic and mesotrophic conditions (i.e., water quality conditions prior to western settlement), we assumed external P loads more typical of oligotrophic and mesotrophic lakes (Table S3 in Supporting Information S1). We ran the model for 300 years, repeating the use of 20 years of driver data, to allow the full system to reach dynamic equilibrium. We then compared water quality metrics with published indices for the different trophic states (Table S4 in Supporting Information S1).

2.4. Legacy Scenarios

We ran three legacy scenarios to investigate the response of Lake Mendota to nutrient load reductions (Table S3 in Supporting Information S1). In our base legacy scenario (Scenario 1), we assumed zero external load of P for 120 years, repeating the same 20 years of hydrology and meteorology used in calibration. We also assumed a 50% reduction in allochthonous OC load and a 50% reduction in inert sediment load that determines P and OC burial rates. In Scenario 2, external P loads were reduced to values typical of mesotrophic lakes, but other conditions were the same as in the base scenario. In Scenario 3, permanent burial rate of sediment P was raised to values assumed for the calibrated model, which provided for a faster water quality recovery than the base scenario.

We tracked all model states and rates through the three scenarios and noted when water quality variables passed thresholds between trophic states (Table S4 in Supporting Information S1). We explored Lake Mendota's memory to historical P loads by comparing the relative rates of change of water quality variables with those of P in the sediments and water column over 120 years. Time series of variables were smoothed with a forward/backward

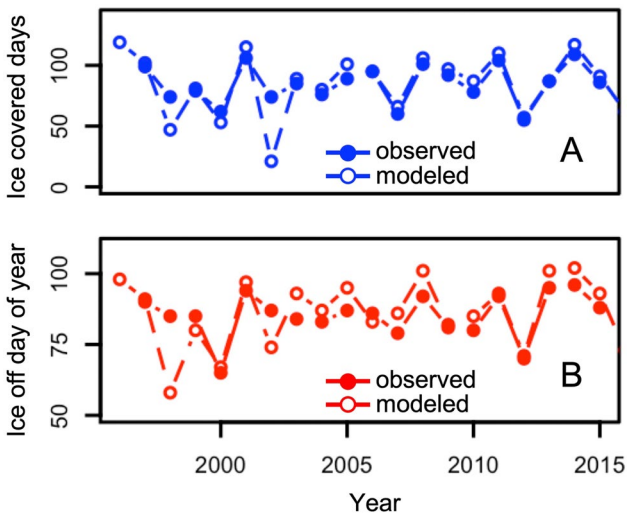

Figure 2. Model results and observational data for lake ice cover for the calibration period. (a) Simulated and observed values for ice covered days each year. The year corresponds to the year that ice-off occurred. (b) Simulated and observed values for ice-off day of year.

moving average filter (10 years) to eliminate interannual variability due to climate and hydrology drivers, and then each time series was normalized to a range of 0–1, with 1 and 0 representing their values at the beginning and end of a scenario, respectively. With these normalized values, we calculated first differences for each variable and divided by the first differences for epilimnetic P and sediment P. A value <1 indicated the variable was lagging (i.e., recovering more slowly than) epilimnetic P change, whereas a value >1 indicated the variable was leading (i.e., recovering more quickly than) epilimnetic P change.

While we used the model to address several questions, we were most interested in understanding why lake water quality responds slowly to nutrient reductions and how Lake Mendota, as a test case, helps us interpret this phenomenon more generally. Thus, a precise estimate of when Lake Mendota might reach an oligotrophic state in the future is less important than understanding how lake processes interact to control the patterns of water quality change we might expect in response to potential nutrient reductions. Through model scenarios, we demonstrate that the general patterns of water quality change are robust to changes in key assumptions about the model and about the lake.

3. Limnological Data and Model Driving Data

Limnological data for calibration were provided by the North Temperate Lakes Long Term Ecological Research program and available in the Environmental Data Initiative repository (Magnuson et al., 2023). These data have been collected fortnightly (every two weeks) or monthly, depending on the variable, since 1995 (Magnuson et al., 2006). Lake sediment core data were used to inform the sediment component of the model (Bortleson & Lee, 1972; Hurley et al., 1992; Lathrop, 2007; Walsh et al., 2019).

Data for driving the model included daily discharge, P and organic carbon (OC) loads, as well as hourly meteorological data. Discharge was taken from Hanson et al. (2020); however, the entire time series was linearly adjusted so that mean hydrologic residence time over the 20-year calibration period of the model was 4.3 years (Lathrop & Carpenter, 2014). Meteorological forcing data were obtained from the second phase of the North American Land Data Assimilation System (Xia et al., 2012). Meteorological variables used in this study included wind speed, air temperature, specific humidity, surface pressure, surface downward short- and longwave radiation, and total precipitation, which were used as boundary data for physical model and metabolism model. Data and model code are published in Hanson (2023).

4. Results

4.1. Comparison of Model Predictions With Observations

The model reproduced well the time dynamics of observed winter ice cover duration, as well as ice-off date (Figure 2). Notable exceptions were 1998 and 2002, when the model over-predicted ice cover duration and ice-off date. The mean observed ice duration was 86 days (±26, 1 SEM), and the mean ice-off day of year 86 (~March 27th), which compared well with the a modeled mean ice duration of 85 days, and modeled mean ice-off day of year 85 (~March 26th). On average, there was less variability among years in the model predictions than in the observations.

Physical and chemical dynamics of the epilimnion and hypolimnion compared well with the observed data (Figures 3a and 3b). The RMSE was 1.28°C and 1.29°C for the epilimnion and hypolimnion, respectively (Table S5 in Supporting Information S1). For Secchi depth, predictions reproduced the observed annual dynamics (Figure 3d), although the RMSE was somewhat high at 2.12 m. Occasional high Secchi values in the observational data were missed by the model. The annual DO cycle was well reproduced for the epilimnion and hypolimnion (Figures 3d and 3e), and RMSE values were 1.45 and 1.97 mg L^{-1}, respectively. Occasional very

21698961, 2023, 12, Downloaded from https://agupubs.onlinelibrary.wiley.com/doi/10.1029/2023JG007620, Wiley Online Library on [12/12/2023]. See the Terms and Conditions (https://onlinelibrary.wiley.com/terms-and-conditions) on Wiley Online Library for rules of use; OA articles are governed by the applicable Creative Commons License

21698961, 2023, 12, Downloaded from https://agupubs.onlinelibrary.wiley.com/doi/10.1029/2023JG007620, Wiley Online Library on [12/12/2023]. See the Terms and Conditions (https://onlinelibrary.wiley.com/terms-and-conditions) on Wiley Online Library for rules of use; OA articles are governed by the applicable Creative Commons License

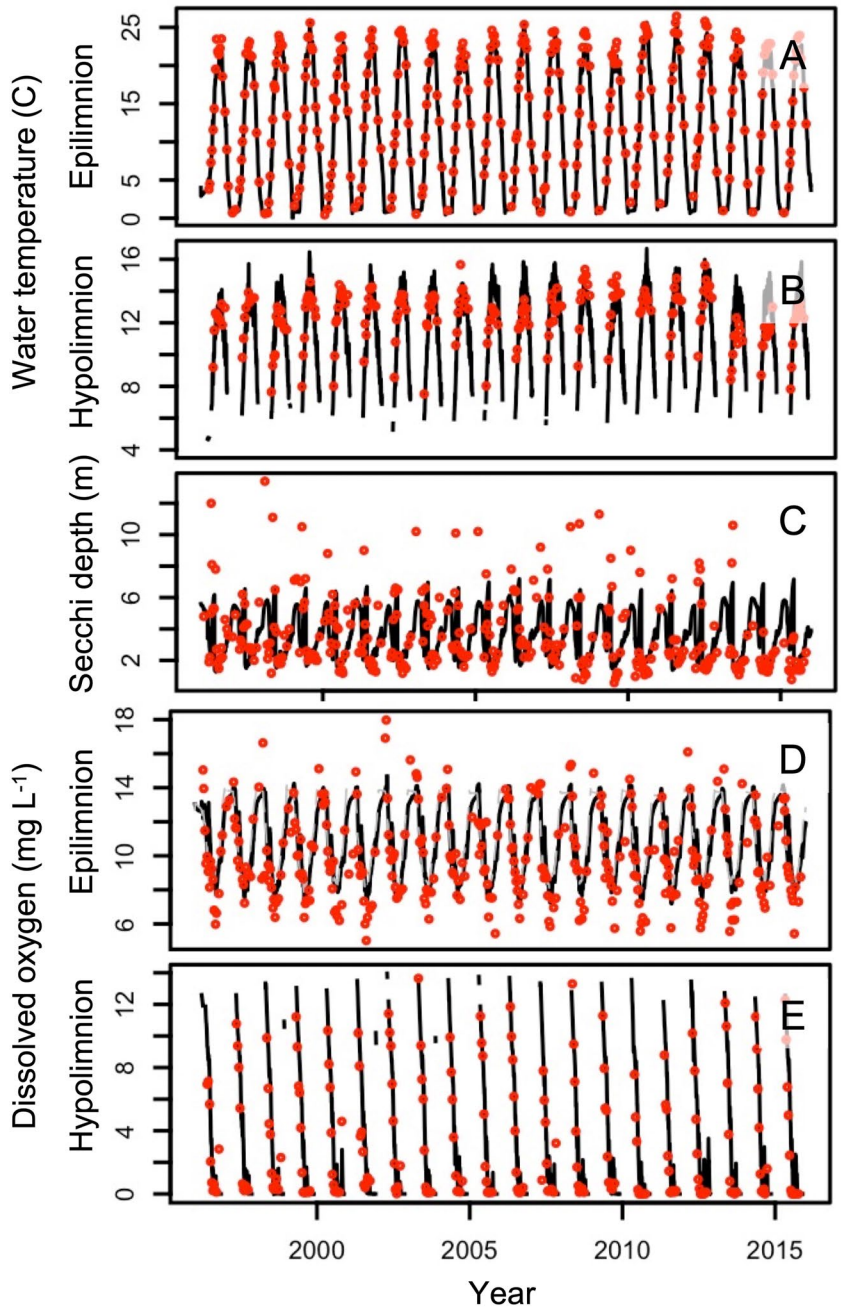

Figure 3. Model predictions (black line) and observations (red circles) for the full calibration period. Panels are (a) water temperature for the epilimnion, and (b) hypolimnion; (c) Secchi depth; (d) dissolved oxygen in the epilimnion, and (e) hypolimnion.

high epilimnetic DO values during winter were missed by the model, and observed values well-below saturation later in summer were missed. We suspect that low observed epilimnetic DO during summer were due to inclusion of the upper half of the metalimnion in the calculation of average epilimnetic DO.

Total phosphorus annual dynamics were reproduced by the model (Figures 4a and 4b). The RMSE values for the epilimnion and hypolimnion were 51.0 and 134 μg L^{-1}, respectively. In general, the model underpredicted epilimnetic annual maxima early in the time series and over-predicted annual maxima late in the time series. Low summer P values were reproduced well, which was an outcome particularly relevant to summertime water quality predictions. The hypolimnetic P predictions matched observations. However, we note the high modeled hypolimnetic P

21698961, 2023, 12, Downloaded from https://agupubs.onlinelibrary.wiley.com/doi/10.1029/2023JG007620, Wiley Online Library on [12/12/2023]. See the Terms and Conditions (https://onlinelibrary.wiley.com/terms-and-conditions) on Wiley Online Library for rules of use; OA articles are governed by the applicable Creative Commons License

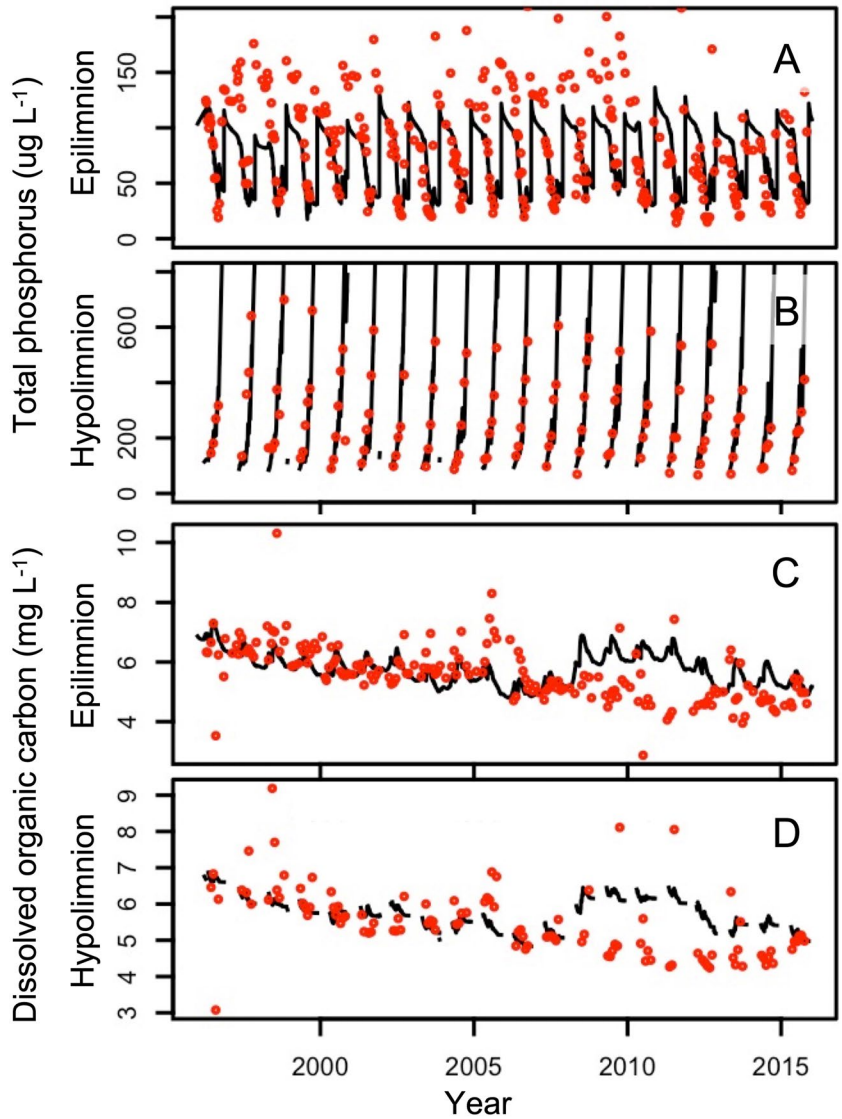

Figure 4. Model predictions (black line) and observations (red circles) for the full calibration period. Panels are (a) total phosphorus for the epilimnion, and (b) hypolimnion; (c) dissolved organic carbon for the epilimnion, and (e) hypolimnion. Four high outlier values in A not shown, and model predictions through the end of the stratified period in B not shown.

concentrations at the end of the stratified period. These concentrations occur after the last observations of the season and cannot be verified due to lack of field data available for this time of year. High P mass in the hypolimnion prior to fall mixis is required to reproduce the observed high water column P immediately following fall mixis.

DOC predictions matched trends of the observations for both the epilimnion and hypolimnion (RMSE of 1.0 and 0.98 mg L^{-1}, respectively). However, the model over-predicted DOC by about 1.5 mg L^{-1} from about 2008 to 2013. We have sparse information on DOC loads, and model deviations from observations may be due to unmeasured changes in the driver data inflow concentrations.

Goodness-of-fit showed mixed results, depending on the test and the state variable (Table S5 in Supporting Information S1). Although NSE was strongly positive for T and DO and slightly positive for Secchi depth, it was negative for epilimnetic P and DOC. KGE, which is thought to be a more reliable statistic for environmental time-series data (Gupta et al., 2009), was positive for all variables. However, KGE for DOC was near zero, suggesting our model for DOC only slightly outperformed a model based on the DOC mean alone.

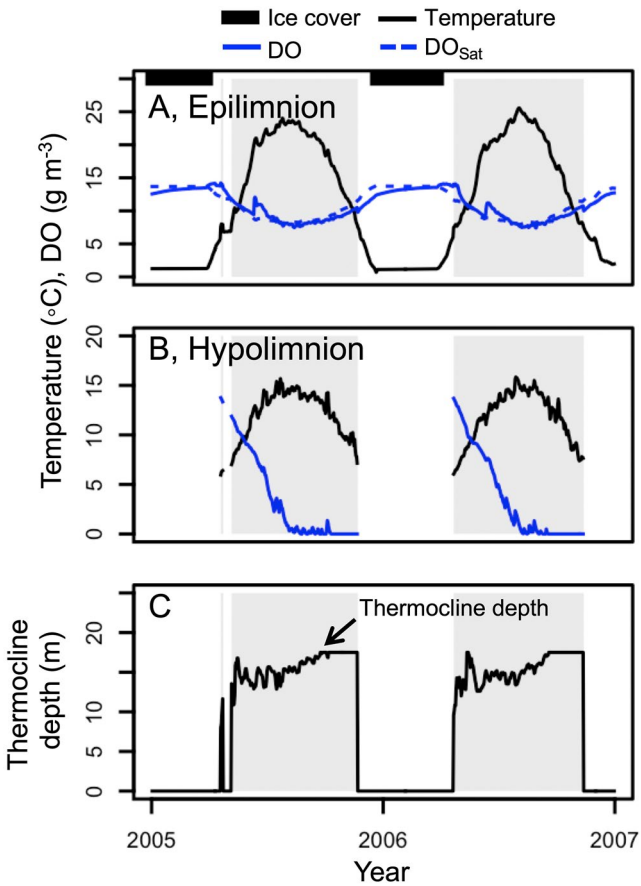

Figure 5. Modeled 2005 and 2006 temperature and dissolved oxygen (DO) for the (a) epilimnion and (b) hypolimnion, and (c) modeled thermocline depth. Periods of ice cover shown in (a). Gray shaded periods represents thermal stratification.

The test of the model using mesotrophic and oligotrophic P load scenarios produced expected water quality behaviors (Figures S1 and S2 in Supporting Information S1). Phosphorus concentrations in the lake decreased to mesotrophic and oligotrophic levels, with annual epilimnetic P ranging from 5 to 100 and 1 to 5 μg L^{-1}, respectively. DOC concentrations in the epilimnion also decreased to mesotrophic and oligotrophic levels, at approximately 4 and 3 mg L^{-1}, respectively. Minimum summer Secchi depth increased to about 2.5 and 5 m for mesotrophic and oligotrophic simulations, respectively. For the mesotrophic simulation, duration of hypolimnetic anoxia decreased by about 10 days y^{-1}; whereas, in the oligotrophic simulation, anoxia no longer occurred.

4.2. Annual Cycles of Temperature, P, OC, and DO

The time dynamics of state variables underlying the water quality of Lake Mendota recreated the expected annual limnological patterns through four distinct seasons. The winter ice-covered period (Figure 5a) had stable physical, chemical and biological conditions relative to other seasons, with low but continuous P settling and P recycling (Figure 6d). Winter productivity was low (Figure 7d), resulting in relatively clear water (Figure 7a). Cold water temperatures drove high annual DO concentrations with oxygen at near saturation (Figure 5a). Spring ice-off was a time of rapid change, with high NPP and increasing settling of both POC (Figures 7d–7f) and P (Figures 6d and 6f). Spring catchment snowmelt and precipitation led to a rise in external P loads (Figure 6d; Figure 7d). Decreasing epilimnetic DO was largely driven by changing temperature (Figure 5a). Water clarity generally decreased in the spring, except during a distinct clear-water phase in late spring (Figure 7a). Thermal stratification began in spring (Figure 5c), along with a rapid decrease in hypolimnetic DO (Figure 5b).

Summer and autumn dynamics had high NPP and POC (algal biomass) (Figure 7d), leading to epilimnetic DO near or above saturation (due to high productivity), despite declining DO solubility as temperatures warmed (Figure 5a). Hypolimnetic DO decreased rapidly after the onset of stable thermal stratification, and the hypolimnion became anoxic (Figure 5b), except for occasional influxes of DO due to short-term variability in the thermocline depth and entrainment of DO-rich water from the epilimnion. High algal biomass resulted in low clarity (Figure 7a). Epilimnetic P decreased to its lowest annual values due to settling out of the epilimnion. Hypolimnetic P became very high (Figures 6a and 6b), due to recycling of P and release of P from the sediments (Figure 6e). Once the hypolimnion became anoxic, mineralization rate of organic P slowed, and the dominant efflux of P from the sediments switched to release of P from the P_B pool in the active sediment layer (Figures 6e and 6f). Autumn turnover triggered the mixing of hypolimnetic nutrients into the entire water column. As P encountered oxic conditions in the surface waters, P rebinding increased, and P settled into the sediments (Figure 6d). Elevated nutrient concentrations supported continued primary production into the autumn (Figure 7d), although rates decreased because of cooling temperatures and reduced irradiance prior to the onset of winter ice cover.

4.3. Major Fluxes and Storage

On an annual basis, most of the P in the water column originated from internal loading from the sediment. Internal P loading (Figures 6d and 6e) was ~5.5 x that of the external load (0.8 gP m^{-2} y^{-1}). Note that in Figure 6d, the large flux of P from the hypolimnion to the epilimnion during fall mixis is not shown, but this accounts for the rapid epilimnetic P increase shown during mixis in Figure 6a. The range of external versus internal loads was relatively narrow across the calibration period, in part because of our model assumptions for external loading, which did not account for changing P concentrations as a function of hydrologic flow.

21698961, 2023, 12, Downloaded from https://agupubs.onlinelibrary.wiley.com/doi/10.1029/2023JG007620, Wiley Online Library on [12/12/2023]. See the Terms and Conditions (https://onlinelibrary.wiley.com/terms-and-conditions) on Wiley Online Library for rules of use; OA articles are governed by the applicable Creative Commons License

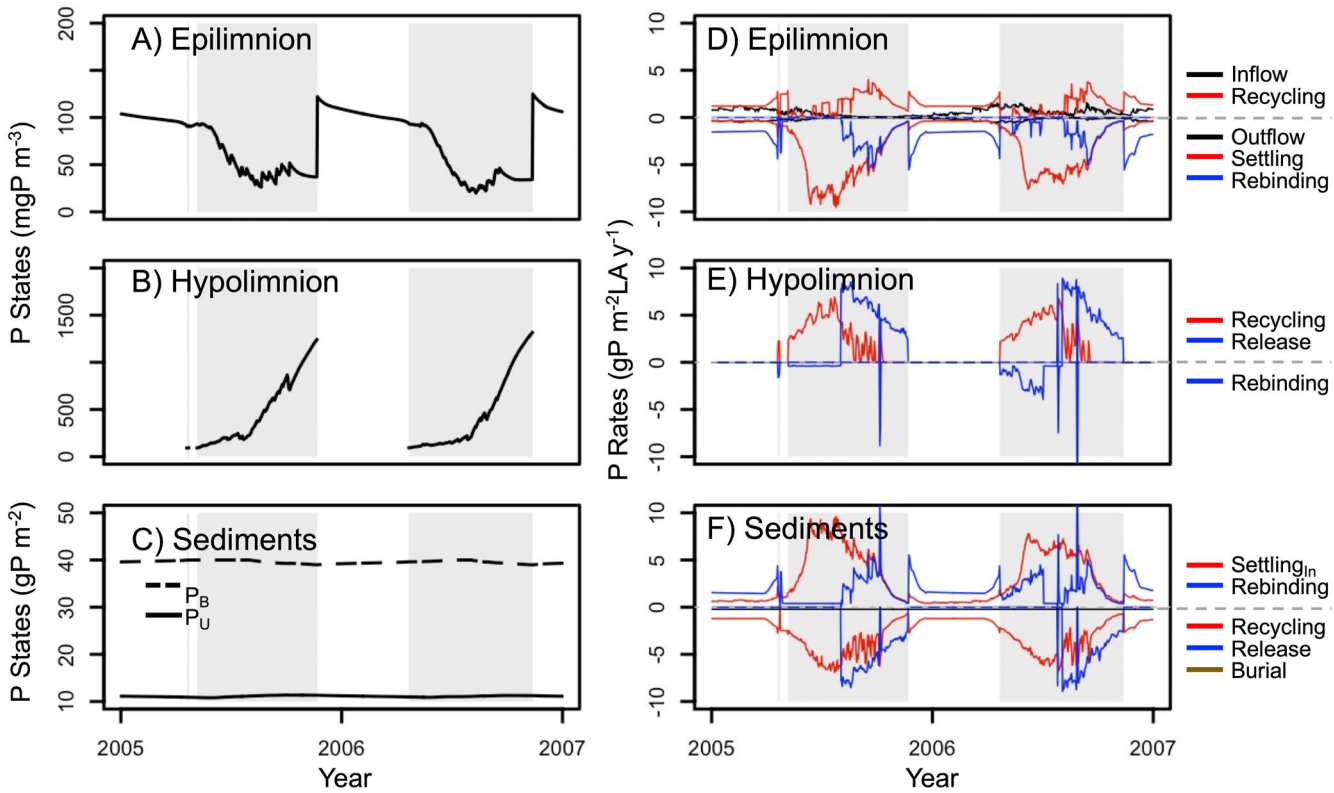

Figure 6. Modeled total phosphorus (P) for 2005 and 2006. (a) P states for the epilimnion, (b) hypolimnion, and (c) sediments. (d) P rates for the epilimnion, (e) hypolimnion, (f) sediments. For rates, paired processes, such as release-rebinding and recycling-settling, are the same color. Positive values are sources and negative values are sinks, with legends above or below zero, respectively. Entrainment not shown. Gray shaded periods represents thermal stratification.

Despite the seasonal variability in water column dynamics, permanent burial of P (Figure 6f) and OC (Figure 7f) in the sediments appeared near constant through the year. This is because sediment concentrations of these constituents are high relative to water column values and therefore have low relative variability (Figures 6c and 7c).

Annual autochthony (i.e., NPP) was much higher than allochthony (Figure 7d). Although most of the autochthony was respired (Figures 7d–7f), a substantial proportion was stored long term in the sediments and buried (Figures 7c and 7f), resulting in long term positive net ecosystem production (NEP) for the lake.

4.4. Legacy Scenarios

Improvement in water quality for Lake Mendota differed depending on the water quality metric and scenario. For Scenario 1 (Figure 8), in which external P loads were set to zero and OC and sediment loads were reduced, epilimnetic P decreased rapidly in the first 20 years due to water column flushing (Figure 8a), followed by a long slow decrease that tracked decreasing hypolimnetic and sediment P (Figures 8b and 8c). For OC, the initial rapid decrease occurred for both the epilimnion and the hypolimnion (Figures 8d and 8e), because the autochthonous pool of OC was produced by epilimnetic NPP. Over the 120 years simulation, sediment OC decreased to roughly half of its original value (Figure 8f). Secchi depth continually increased following decreases in OC (Figure 8g). Dissolved oxygen was the variable slowest to respond to reduced external loads. Although sediment oxygen demand decreased linearly (Figure 8h), the number of anoxic days decreased slowly for about 50 years, and then decreased rapidly until about year 95, at which time anoxia no longer occurred (Figure 8i). The annual range for P and POC decreased with the decreasing mean value. For Secchi depth, the range decreased with increasing value.

Overall, the pathways to improved trophic states differed among variables after external loads were set to zero (Figure 9). Light extinction, which is inversely related to Secchi depth, and epilimnetic P passed the eutrophic-mesotrophic threshold between years 10–15 of the simulation. Epilimnetic P passed the mesotrophic-oligotrophic threshold at year ~40, while light extinction passed that threshold about 35 years later.

21698961, 2023, 12, Downloaded from https://agupubs.onlinelibrary.wiley.com/doi/10.1029/2023JG007620, Wiley Online Library on [12/12/2023]. See the Terms and Conditions (https://onlinelibrary.wiley.com/terms-and-conditions) on Wiley Online Library for rules of use; OA articles are governed by the applicable Creative Commons License

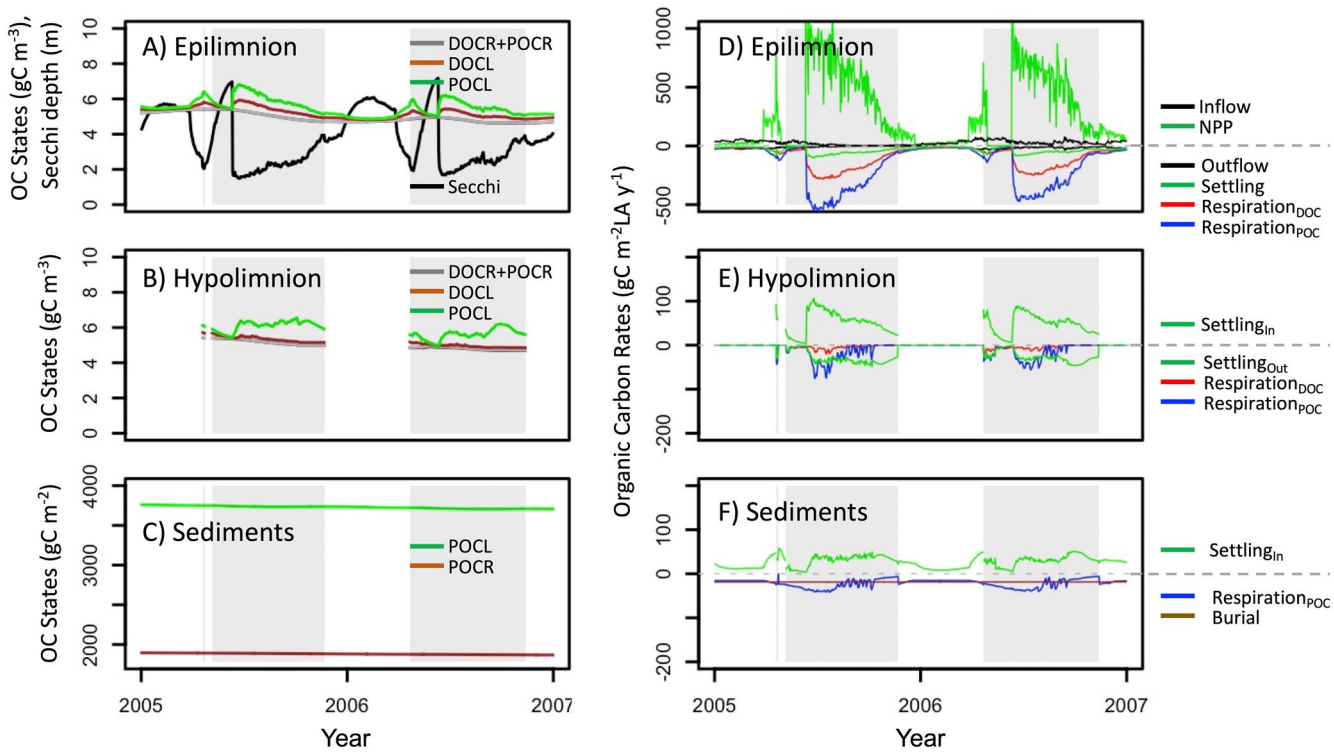

Figure 7. Modeled organic carbon and Secchi depth for 2005 and 2006. Lines for OC are stacked. (a) Organic carbon states and Secchi depth for the epilimnion, (b) organic carbon states for the hypolimnion, and (c) sediments. (d) Organic carbon rates for the epilimnion, (e) hypolimnion, (f) sediments. For rates, positive values are sources and negative values are sinks, with legends above or below zero, respectively. Lines are not stacked for d–f. Inflow and outflow are total organic carbon, settling is all forms of POC, and respiration includes both labile and refractory forms combined. Burial is all POC. Gray shaded areas represents thermal stratification.

The duration of anoxia showed a different pattern, which was convex until about year 60 of the simulation. Although there was a steady decrease in anoxia over time, anoxic days did not drop to mesotrophic levels until year ~85 of the simulation and did not drop to oligotrophic values (i.e., disappear) until year ~95.

Scenarios 2 and 3 (Figures S3, S4, S5, and S6 in Supporting Information S1) showed the same general patterns as Scenario 1, but with differing rates. For Scenario 2 (mesotrophic P loads), water quality values never passed the threshold from eutrophic to mesotrophic. The duration of the scenario, set to 120 years, was simply too short. In contrast, Scenario 3 (high inert sediment load and burial rate) demonstrated the importance of higher burial rates in the sediment nutrient and carbon budgets. When burial rate was high, water quality improvement occurred ~25% more quickly overall.

To quantify lags between changes in lake P and water quality responses, we calculated the relative annual rates of change for variables over the simulation period (Figures 9b and 9c). Until about year 20, all metrics lagged (changed at a lower relative rate) changes in epilimnetic P concentrations (Figure 9b). At 20 years, POC_{Epi} and sediment oxygen demand led (changed at a higher relative rate) P_{Epi}. Light extinction and anoxic days changed from lagging P_{Epi} to leading P_{Epi} at about year 50. When compared to sediment P (Figure 9c), only sediment O_2 demand and anoxic days lagged P_{Sed} changes initially. Other metrics (P_{Epi}, POC_{Epi}, light extinction), which respond to water column flushing, led P_{Sed} until about year 20. All metrics, other than P_{Epi}, lagged P_{Sed} until about years 50–70. P_{Epi} continued to lag P_{Sed} through the end of the simulation.

5. Discussion

5.1. Legacies of Eutrophication for Lake Mendota

The legacy of more than a century of high nutrient loads to Lake Mendota is degraded water quality that persists for decades to longer than a century under the most aggressive nutrient reduction scenario. Fundamentally, a century of water quality degradation requires a century (or longer) of recovery. Although initial improvement in

21698961, 2023, 12, Downloaded from https://agupubs.onlinelibrary.wiley.com/doi/10.1029/2023JG007620, Wiley Online Library on [12/12/2023]. See the Terms and Conditions (https://onlinelibrary.wiley.com/terms-and-conditions) on Wiley Online Library for rules of use; OA articles are governed by the applicable Creative Commons License

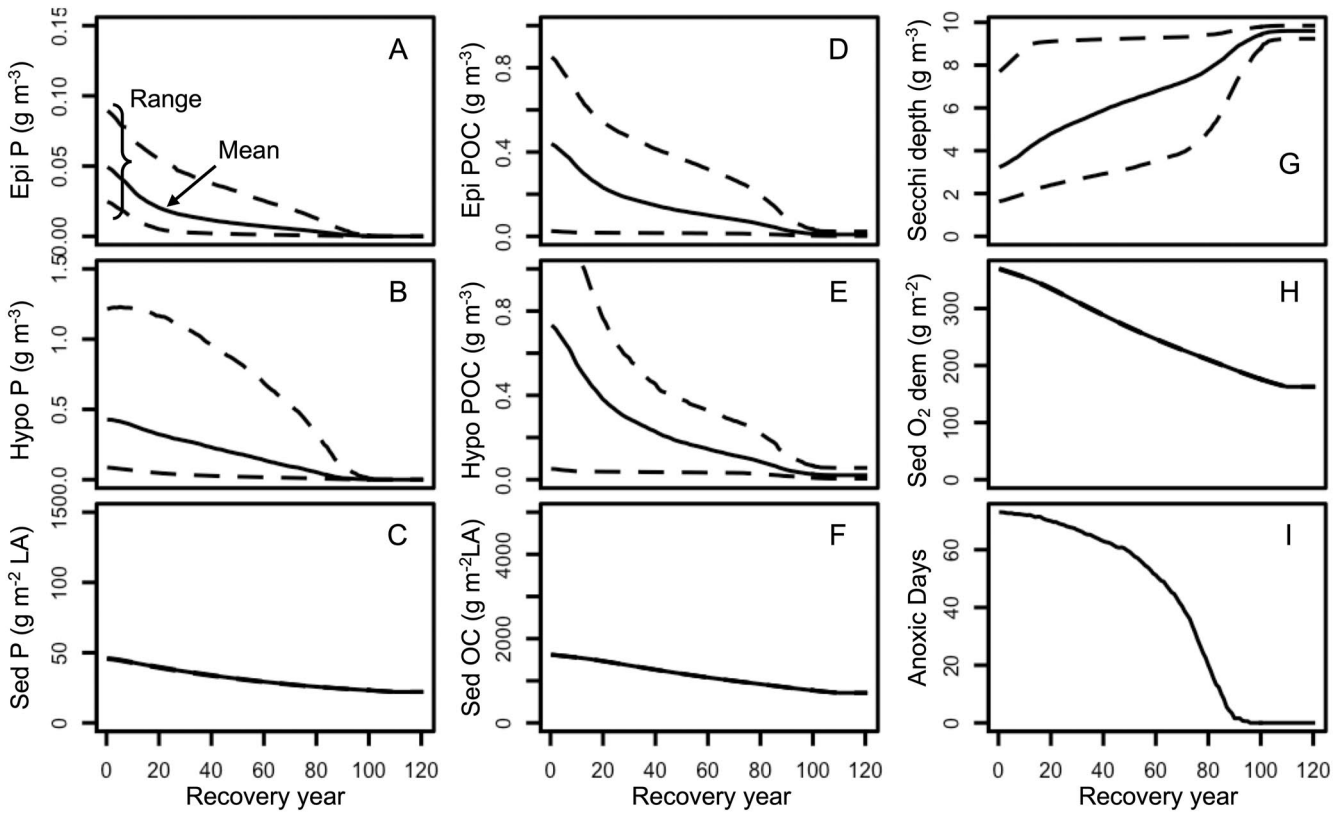

Figure 8. Recovery of water quality metrics following cessation of external P inputs. Data are smoothed annual means. Dashed lines indicate annual range. (a–c) Ecosystem total P. (d–e) Total POC in the water column and (f) sediments. (g) Secchi depth, (h) Sediment oxygen demand, and (i) anoxic days during.

water clarity and epilimnetic P may occur in a couple of decades, high internal nutrient loads will continue to fuel elevated primary production for a century. The long and slow response of water quality to nutrient reduction has been shown empirically for other lakes (Jeppesen et al., 2005; Søndergaard et al., 2013). For Lake Mendota, we have demonstrated how nutrient cycling and lake metabolism interact to control how water quality responds to both the reduction of external loads and the long and slow depletion of sediment nutrient stocks.

Phosphorus stored in the sediments of Lake Mendota controlled the bottom-up response of water quality to nutrient load reductions. At approximately 125 g P m^{-2} of active sediment area, a typical sediment P density for eutrophic lakes (Carey & Rydin, 2011), the sediment pool has approximately two orders of magnitude more P than the annual average water column value of ~1.0 g P m^{-2}. Given Lake Mendota's hydrologic residence time of ~4 years and typical water column P concentrations, only ~0.25 g P m^{-2} at most can be flushed annually from the water column, assuming no additional external loads. Thus, a ~30% reduction in the sediment pool needed for the lake to return to a mesotrophic state would take about 150 years through the process of flushing alone. These findings support previous work that eutrophication persists in lakes long-term, despite P remediation (Søndergaard et al., 2007, 2013). However, deposition of sediments that may bind P or bury it in sediments (Rothe et al., 2014) accelerates the recovery process, because permanent burial can be an important sink in the sediment P mass balance (Carleton & Lee, 2023). The high inert sediment load in Scenario 3 (Figure S6 in Supporting Information S1) emphasizes the importance of burial to sediment P reduction and subsequent water column improvement.

5.2. Ecosystem Memory and Surprises on the Path to Trophic State Improvement

Ecosystem memory slowed the response of water quality to nutrient load reductions in Lake Mendota. Water clarity and DO improvement lagged the long, slow decline in sediment P because of the lags associated with the coupled dynamics of P-cycling, metabolism, and DO. Although water column P may change rapidly due to reduced external loads, the fraction of water column P derived from internal loads will lag sediment P decreases because of the lake's hydrologic residence time. Lake water quality is linked to water column P

21698961, 2023, 12, Downloaded from https://agupubs.onlinelibrary.wiley.com/doi/10.1029/2023JG007620, Wiley Online Library on [12/12/2023]. See the Terms and Conditions (https://onlinelibrary.wiley.com/terms-and-conditions) on Wiley Online Library for rules of use; OA articles are governed by the applicable Creative Commons License

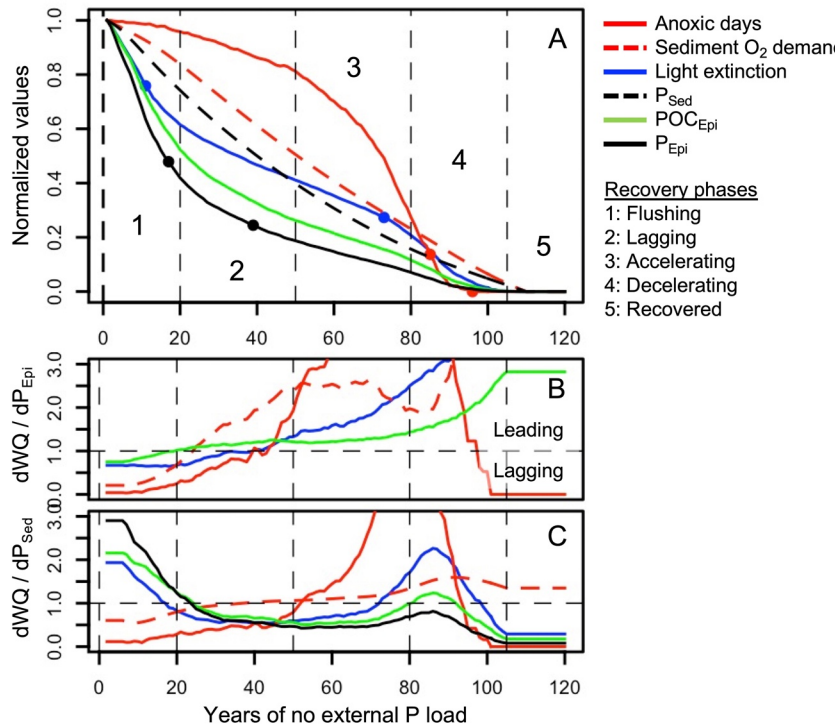

Figure 9. (a) Response pathways for metrics of water quality. Water quality metrics normalized to a range of 0–1, with high values representing initial conditions and zero representing values at 120 years following cessation of external P loads. Circles on P_{epi}, light extinction, and anoxic days represent trophic thresholds, based on values before normalization. Earlier values are eutrophic to mesotrophic thresholds, and later values are mesotrophic to oligotrophic thresholds. Numbers in boxes are recovery phases. (b) Change in water quality metrics with respect to change in mean surface P and (c) sediment P. Horizontal line at $y = 1$ separates a lagged response in water quality (<1) from an accelerated response (>1).

through metabolism, and a change in water quality, such as hypolimnetic anoxia, requires a shift in metabolic balance that may not be realized until water column P is greatly reduced. Our expectation was that all water quality metrics would improve following cessation of external loads in the legacy scenarios, even if the rate of improvement was slower than that of P in the water column. However, the rate of change in hypolimnetic anoxia initially remained nearly flat as the annual duration of hypolimnetic anoxia showed minimal improvement for nearly two decades (Figure 9). In Scenario 2 (60% reduction in P load), which arguably would be a more likely "real-world" scenario, the duration of anoxia actually became worse for the first decade. This surprising outcome was due to changes in the sediment OC mass balance. When allochthony was turned off, sediment deposition decreased in our model, reducing permanent burial rates for P and OC. For the first 1–2 decades of recovery, water column P was still at concentrations high enough to support high production of autochthonous POC (positive NEP), which kept the sediment OC mass balance near neutral in Scenario 1 and positive (i.e., accumulation of sediment OC) in Scenario 2. At about year 20 of recovery, sediment P diminished to the point where P recycled to the water column was lower, and NPP and POC were sufficiently reduced to tip the sediment mass balance toward a reduction in POC. In general, consumption of hypolimnetic O_2 depends on a number of factors, including lake morphometry (Steinsberger et al., 2020), climate variability (Ladwig et al., 2021; Snortheim et al., 2017), and water column stability (Ladwig et al., 2021), but chiefly the OC available as substrate for microbial respiration and the benthic flux of reduced substances (Müller et al., 2012). Once NEP in the water column became negative (i.e., lower export of POC to the sediments), sediment O_2 demand and anoxic days diminished.

Linked cycles of P, OC, and DO produce nested lags in the response times of water quality metrics to reduced nutrient loads and provide a mechanistic basis for ecosystem memory. The recovery to an improved trophic state of some water quality metrics can only occur following substantial changes in other nutrient or carbon pools. For example, elimination of hypolimnetic anoxia requires depletion of the OC available for respiration, and depletion of OC lags recovery of P by several decades because of the influence of P on autochthony and NEP (i.e., lake

21698961, 2023, 12, Downloaded from https://agupubs.onlinelibrary.wiley.com/doi/10.1029/2023JG007620, Wiley Online Library on [12/12/2023]. See the Terms and Conditions (https://onlinelibrary.wiley.com/terms-and-conditions) on Wiley Online Library for rules of use; OA articles are governed by the applicable Creative Commons License

21698961, 2023, 12, Downloaded from https://agupubs.onlinelibrary.wiley.com/doi/10.1029/2023JG007620, Wiley Online Library on [12/12/2023]. See the Terms and Conditions (https://onlinelibrary.wiley.com/terms-and-conditions) on Wiley Online Library for rules of use; OA articles are governed by the applicable Creative Commons License

metabolism). Lake metabolism is sensitive to long-term lake changes (e.g., Richardson et al., 2017), highlighting its utility for tracking coupled biological and chemical water quality responses to external loading.

Differing lags of recovery explain why different water quality metrics pass inter-trophic thresholds at different times (Figure 9). During recovery in Scenario 1, water clarity, based on POC concentration (i.e., algal biomass in this model), lags P recovery by about 30 years, and hypolimnetic oxygen lags water clarity by about 20 years. Thus, transitioning to an oligotrophic state can vary in time from about 40 to 95 years, depending on the water quality metric. Nonetheless, the sequence of responses from decreasing P to improved oxic condition pass through a set of predictable phases, described below.

5.3. Phases of Water Quality Improvement

Our scenarios reveal five distinct phases of water quality improvement (Figure 9). The phases are identified visually, based on changes in water quality metrics relative to P_{Epi} (Figure 9b), which is more easily measured in lakes than sediment P. The first phase is water column flushing, which corresponds to a rapid decrease in solutes as external loads of P and OC are eliminated and reduced, respectively. In Phase 2, water quality metrics lag changes in P_{Epi}. In Phase 3, improvement in water quality metrics accelerates relative to P_{Epi} and then decelerates in Phase 4 as all variables approach a new dynamic equilibrium in the oligotrophic state. In Phase 5, water quality metrics have reached their oligotrophic values.

The long time period needed for transitions across these five phases provides context for localized ecosystem behavior that otherwise might appear puzzling within the time frame of short-term monitoring programs. Any initial rapid improvement in water quality will stall following water column flushing. Further improvement in water quality will proceed more slowly than declining P_{Epi} (i.e., values <1 in Figure 9b) for decades. Eventually, water quality will improve more rapidly than P_{Epi} (i.e., values >1 in Figure 9b) until the system reaches its improved trophic state. In Lake Mendota, these phases would play out over decades and could be observed only through long-term monitoring. We expect that this behavior likely would be applicable to other eutrophic lakes with similar external loading history, although this remains unknown and motivates future work. Altogether, a long view that incorporates ecosystem memory is required to understand localized ecosystem behavior during remediation of degraded water quality.

5.4. Caveats

Two assumptions in our model regarding sediment P pools are especially worthy of further consideration for analyzing Mendota patterns and scaling these results to other lakes. First, the model sets sediment P binding capacity at 1 mg P per gram dry sediment, based on empirical measures of sediment total P concentrations in Lake Mendota (Hoffman et al., 2013). Although this static threshold works well in the model, the reality of sediment P sorption capacity is far more complex and may depend on factors such as changes in particle size and mineralogy of deposited sediments (Stone & English, 1993). Along with hypolimnetic dissolved oxygen status, the binding capacity parameter determines the rate at which P may re-bind to the mineral P pool in the sediments and influences the balance of sediment P retention versus release. As such, the model would benefit from further exploration of this parameter, including options for dynamic P binding capacity over time. Second, the model focuses primarily on redox-sensitive P minerals (iron- and manganese-bound P) in the bound sediment P pool, which is supported by empirical evidence of the importance of anoxic internal P loading in Lake Mendota (Hoffman et al., 2013). However, mineral sediment P may be associated with other metals, such as aluminum and calcium, which are generally considered less mobile than redox-sensitive P forms (Orihel et al., 2017), and are not explicitly represented in our model. Conversely, co-precipitation of soluble phosphorus with calcite may be another pathway for P burial in Lake Mendota (Gonsiorczyk et al., 1998; Reddy et al., 2021), motivating future work on linked calcium and P cycling, as well as more detailed P speciation modeling, in Lake Mendota.

Additionally, application of the modeling approach to other waterbodies may require consideration of legacy N pools and cycling. We focused our assessment of nutrient cycling on P due to evidence of P limitation in Lake Mendota (Lathrop, 2007) as well as numerous case studies of P control eliciting desirable water quality responses (Schindler et al., 2016). This assumption was supported by good model performance compared to the long-term observational data. However, model application to N-limited waterbodies will require consideration of N cycling as legacy N loads likely play an important role in long-term lake functioning in these systems.

21698961, 2023, 12, Downloaded from https://agupubs.onlinelibrary.wiley.com/doi/10.1029/2023JG007620, Wiley Online Library on [12/12/2023]. See the Terms and Conditions (https://onlinelibrary.wiley.com/terms-and-conditions) on Wiley Online Library for rules of use; OA articles are governed by the applicable Creative Commons License

Repairing ecosystems usually requires more time and effort than damaging them (Jones et al., 2018), in part due to long ecosystem memory. Lake Mendota was eutrophied over a relatively short time period—probably less than 100 years and has likely had an anoxic hypolimnion as far back as the early 1900s (Lathrop, 2007). Our simulations indicate a return to pre-European settlement conditions using external P reduction alone will take decades, if not centuries. Interaction of cycles in Lake Mendota underlie that long memory, leading to long delays between external P load reduction and water quality improvement, because available P must be reduced sufficiently to tip the ecosystem OC balance toward net mineralization rather than net accumulation. Only then can microbes begin to consume the organic matter of past decades and slowly eliminate the substrate that fuels anoxia. This takes time and the will of a society to undergo a multi-generational remediation of a precious water resource.

Data Availability Statement

All data and software for this project are open and freely available through the Environmental Data Initiative (Hanson, 2023). Data and software are licensed as Creative Commons Attribution 4.0 International.

Acknowledgments
This work benefitted from decades of research and monitoring by the North Temperate Lakes Long Term Ecological Research program (NSF 2025982). We thank Sylvia Lee and James Carleton for inspiration in pursuing these ideas. Funding support for PCH provided by NSF 2213549, NSF 1753657. Funding support for CCC provided by NSF 1753639, NSF 1933016, NSF 1926050, NSF 2213550. Funding support for RL and CB provided by NSF 1759865, NSF 1934633. Funding support for EAA provided by NSF GRFP DGE-1747503, with additional Support from the Graduate School and the Office of the Vice Chancellor for Research and Graduate Education at the University of Wisconsin-Madison with funding from the Wisconsin Alumni Research Foundation.

References

Albright, E. A., Ladwig, R., & Wilkinson, G. M. (2022). Influence of macrophytes on stratification and dissolved oxygen dynamics in ponds. Retrieved from https://eartharxiv.org/repository/view/3613/

Bennett, E. M., Reed-Andersen, T., Houser, J. N., Gabriel, J. R., & Carpenter, S. R. (1999). A phosphorus budget for the Lake Mendota watershed. *Ecosystems*, *2*(1), 69–75. https://doi.org/10.1007/s100219900059

Bortleson, G. C., & Lee, G. F. (1972). Recent sedimentary history of Lake Mendota, Wis. *Environmental Science & Technology*, *6*(9), 799–808. https://doi.org/10.1021/es60068a002

Brock, T. D. (1985). *A eutrophic lake: Lake Mendota, Wisconsin* (Vol. 55). Springer Science & Business Media.

Carey, C. C., Doubek, J. P., McClure, R. P., & Hanson, P. C. (2018). Oxygen dynamics control the burial of organic carbon in a eutrophic reservoir. *Limnology and Oceanography Letters*, *3*(3), 293–301. https://doi.org/10.1002/lol2.10057

Carey, C. C., & Rydin, E. (2011). Lake trophic status can be determined by the depth distribution of sediment phosphorus. *Limnology & Oceanography*, *56*(6), 2051–2063. https://doi.org/10.4319/lo.2011.56.6.2051

Carleton, J. N., & Lee, S. S. (2023). Estimating lake recovery lag times following influent phosphorus loading reduction. *Environmental Modelling & Software*, *162*, 105642. https://doi.org/10.1016/j.envsoft.2023.105642

Carpenter, S. R., & Bennett, E. M. (2011). Reconsideration of the planetary boundary for phosphorus. *Environmental Research Letters*, *6*(1), 014009. https://doi.org/10.1088/1748-9326/6/1/014009

Chen, S., Carey, C. C., Little, J. C., Lofton, M. E., McClure, R. P., & Lei, C. (2018). Effectiveness of a bubble-plume mixing system for managing phytoplankton in lakes and reservoirs. *Ecological Engineering*, *113*, 43–51. https://doi.org/10.1016/j.ecoleng.2018.01.002

Damania, R., Desbureaux, S., Rodella, A.-S., Russ, J., & Zaveri, E. (2019). *Quality unknown: The invisible water crisis*. The World Bank.

Faridmarandi, S., Khare, Y. P., & Naja, G. M. (2020). Long-term regional nutrient contributions and in-lake water quality trends for Lake Okeechobee. *Lake and Reservoir Management*, *37*(1), 77–94. https://doi.org/10.1080/10402381.2020.1809036

Folke, C., Carpenter, S. R., Chapin, F. S., III, Gaffney, O., Galaz, V., Hoffmann, H., et al. (2020). *Our future in the anthropocene biosphere: Global sustainability and resilient societies*. Folke.

Gonsiorczyk, T., Casper, P., & Koschel, R. (1998). Phosphorus-binding forms in the sediment of an oligotrophic and an eutrophic hardwater lake of the Baltic Lake District (Germany). *Water Science and Technology*, *37*(3), 51–58. https://doi.org/10.2166/wst.1998.0173

Gupta, H. V., Kling, H., Yilmaz, K. K., & Martinez, G. F. (2009). Decomposition of the mean squared error and NSE performance criteria: Implications for improving hydrological modelling. *Journal of Hydrology*, *377*(1–2), 80–91. https://doi.org/10.1016/j.jhydrol.2009.08.003

Hanson, P. C. (2023). Lake Mendota long term water quality model [Dataset]. EDI. https://doi.org/10.6073/pasta/f21259ba038cb517b876131b2fda41a1

Hanson, P. C., Bade, D. L., Carpenter, S. R., & Kratz, T. K. (2003). Lake metabolism: Relationships with dissolved organic carbon and phosphorus. *Limnology & Oceanography*, *48*(3), 1112–1119. https://doi.org/10.4319/lo.2003.48.3.1112

Hanson, P. C., Stillman, A. B., Jia, X., Karpatne, A., Dugan, H. A., Carey, C. C., et al. (2020). Predicting lake surface water phosphorus dynamics using process-guided machine learning. *Ecological Modelling*, *430*, 109136. https://doi.org/10.1016/j.ecolmodel.2020.109136

Hoellein, T. J., Bruesewitz, D. A., & Richardson, D. C. (2013). Revisiting Odum (1956): A synthesis of aquatic ecosystem metabolism. *Limnology & Oceanography*, *58*(6), 2089–2100. https://doi.org/10.4319/lo.2013.58.6.2089

Hoffman, A. R., Armstrong, D. E., & Lathrop, R. C. (2013). Influence of phosphorus scavenging by iron in contrasting dimictic lakes. *Canadian Journal of Fisheries and Aquatic Sciences*, *70*(7), 941–952. https://doi.org/10.1139/cjfas-2012-0391

Hotchkiss, E. R., Sadro, S., & Hanson, P. C. (2018). Toward a more integrative perspective on carbon metabolism across lentic and lotic inland waters. *Limnology and Oceanography Letters*, *3*(3), 57–63. https://doi.org/10.1002/lol2.10081

Hurley, J. P., Armstrong, D. E., & DuVall, A. L. (1992). Historical interpretation of pigment stratigraphy in Lake Mendota sediments. In *Food web management* (pp. 49–68). Springer.

Jenny, J., Francus, P., Normandeau, A., Lapointe, F., Perga, M., Ojala, A., et al. (2016). Global spread of hypoxia in freshwater ecosystems during the last three centuries is caused by rising local human pressure. *Global Change Biology*, *22*(4), 1481–1489. https://doi.org/10.1111/gcb.13193

Jeppesen, E., Søndergaard, M., Jensen, J. P., Havens, K. E., Anneville, O., Carvalho, L., et al. (2005). Lake responses to reduced nutrient loading–an analysis of contemporary long-term data from 35 case studies. *Freshwater Biology*, *50*(10), 1747–1771. https://doi.org/10.1111/j.1365-2427.2005.01415.x

Jones, H. P., Jones, P. C., Barbier, E. B., Blackburn, R. C., Rey Benayas, J. M., Holl, K. D., et al. (2018). Restoration and repair of Earth's damaged ecosystems. *Proceedings of the Royal Society B: Biological Sciences*, *285*(1873), 20172577. https://doi.org/10.1098/rspb.2017.2577

Keatley, B. E., Bennett, E. M., MacDonald, G. K., Taranu, Z. E., & Gregory-Eaves, I. (2011). Land-use legacies are important determinants of lake eutrophication in the anthropocene. *PLoS One*, *6*(1), e15913. https://doi.org/10.1371/journal.pone.0015913

Kothawala, D. N., Stedmon, C. A., Müller, R. A., Weyhenmeyer, G. A., Köhler, S. J., & Tranvik, L. J. (2014). Controls of dissolved organic matter quality: Evidence from a large-scale boreal lake survey. *Global Change Biology*, *20*(4), 1101–1114. https://doi.org/10.1111/gcb.12488

Ladwig, R., Appling, A. P., Delany, A., Dugan, H. A., Gao, Q., Lottig, N., et al. (2022). Long-term change in metabolism phenology in north temperate lakes. *Limnology & Oceanography*, *67*(7), 1502–1521. https://doi.org/10.1002/lno.12098

Ladwig, R., Hanson, P. C., Dugan, H. A., Carey, C. C., Zhang, Y., Shu, L., et al. (2021). Lake thermal structure drives interannual variability in summer anoxia dynamics in a eutrophic lake over 37 years. *Hydrology and Earth System Sciences*, *25*(2), 1009–1032. https://doi.org/10.5194/hess-25-1009-2021

Lathrop, R. C. (2007). Perspectives on the eutrophication of the Yahara lakes. *Lake and Reservoir Management*, *23*(4), 345–365. https://doi.org/10.1080/07438140709354023

Lathrop, R. C., & Carpenter, S. R. (2014). Water quality implications from three decades of phosphorus loads and trophic dynamics in the Yahara chain of lakes. *Inland Waters*, *4*(1), 1–14. https://doi.org/10.5268/iw-4.1.680

Lee, M., & Diop, S. (2009). Millennium ecosystem assessment. *An Assessment of Assessments: Findings of the Group of Experts Pursuant to UNGA Resolution 60/30*, *1*, 361.

Magnuson, J. J., Carpenter, S. R., & Stanley, E. H. (2023). North temperate lakes LTER: Chemical limnology of primary study lakes: Nutrients, pH and carbon 1981—Current ver 59 [Dataset]. Environmental Data Initiative. https://doi.org/10.6073/pasta/c923b8e044310f3f5612dab09c2cc6c2

Magnuson, J. J., Kratz, T. K., & Benson, B. J. (2006). *Long-term dynamics of lakes in the landscape: Long-term ecological research on north temperate lakes*. Oxford University Press on Demand.

Matzinger, A., Müller, B., Niederhauser, P., Schmid, M., & Wüest, A. (2010). Hypolimnetic oxygen consumption by sediment-based reduced substances in former eutrophic lakes. *Limnology & Oceanography*, *55*(5), 2073–2084. https://doi.org/10.4319/lo.2010.55.5.2073

McCrackin, M. L., Jones, H. P., Jones, P. C., & Moreno-Mateos, D. (2017). Recovery of lakes and coastal marine ecosystems from eutrophication: A global meta-analysis. *Limnology & Oceanography*, *62*(2), 507–518. https://doi.org/10.1002/lno.10441

Missimer, T. M., Thomas, S., & Rosen, B. H. (2020). Legacy phosphorus in Lake Okeechobee (Florida, USA) sediments: A review and new perspective. *Water*, *13*(1), 39. https://doi.org/10.3390/w13010039

Müller, B., Bryant, L. D., Matzinger, A., & Wüest, A. (2012). Hypolimnetic oxygen depletion in eutrophic lakes. *Environmental Science & Technology*, *46*(18), 9964–9971. https://doi.org/10.1021/es301422r

Odum, H. T. (1956). Primary production in flowing waters 1. *Limnology & Oceanography*, *1*(2), 102–117. https://doi.org/10.4319/lo.1956.1.2.0102

Ogle, K., Barber, J. J., Barron-Gafford, G. A., Bentley, L. P., Young, J. M., Huxman, T. E., et al. (2015). Quantifying ecological memory in plant and ecosystem processes. *Ecology Letters*, *18*(3), 221–235. https://doi.org/10.1111/ele.12399

Oliver, S. K., Collins, S. M., Soranno, P. A., Wagner, T., Stanley, E. H., Jones, J. R., et al. (2017). Unexpected stasis in a changing world: Lake nutrient and chlorophyll trends since 1990. *Global Change Biology*, *23*(12), 5455–5467. https://doi.org/10.1111/gcb.13810

Orihel, D. M., Baulch, H. M., Casson, N. J., North, R. L., Parsons, C. T., Seckar, D. C., & Venkiteswaran, J. J. (2017). Internal phosphorus loading in Canadian fresh waters: A critical review and data analysis. *Canadian Journal of Fisheries and Aquatic Sciences*, *74*(12), 2005–2029. https://doi.org/10.1139/cjfas-2016-0500

Paraska, D. W., Hipsey, M. R., & Salmon, S. U. (2014). Sediment diagenesis models: Review of approaches, challenges and opportunities. *Environmental Modelling & Software*, *61*, 297–325. https://doi.org/10.1016/j.envsoft.2014.05.011

Reddy, K., Hu, J., Villapando, O., Bhomia, R. K., Vardanyan, L., & Osborne, T. (2021). Long-term accumulation of macro-and secondary elements in subtropical treatment wetlands. *Ecosphere*, *12*(11), e03787. https://doi.org/10.1002/ecs2.3787

Richardson, D., Melles, S., Pilla, R., Hetherington, A., Knoll, L., Williamson, C., et al. (2017). Transparency, geomorphology and mixing regime explain variability in trends in lake temperature and stratification across Northeastern North America (1975–2014). *Water*, *9*(6), 442. https://doi.org/10.3390/w9060442

Rothe, M., Frederichs, T., Eder, M., Kleeberg, A., & Hupfer, M. (2014). Evidence for vivianite formation and its contribution to long-term phosphorus retention in a recent lake sediment: A novel analytical approach. *Biogeosciences*, *11*(18), 5169–5180. https://doi.org/10.5194/bg-11-5169-2014

Sabo, R. D., Clark, C. M., Gibbs, D. A., Metson, G. S., Todd, M. J., LeDuc, S. D., et al. (2021). Phosphorus inventory for the conterminous United States (2002–2012). *Journal of Geophysical Research: Biogeosciences*, *126*(4), e2020JG005684. https://doi.org/10.1029/2020jg005684

Scheffer, M., Carpenter, S., Foley, J. A., Folke, C., & Walker, B. (2001). Catastrophic shifts in ecosystems. *Nature*, *413*(6856), 591–596. https://doi.org/10.1038/35098000

Schindler, D. W., Carpenter, S. R., Chapra, S. C., Hecky, R. E., & Orihel, D. M. (2016). Reducing phosphorus to curb lake eutrophication is a success. *Environmental Science & Technology*, *50*(17), 8923–8929. https://doi.org/10.1021/acs.est.6b02204

Sharpley, A., Helmers, M. J., Kleinman, P., King, K., Leytem, A., & Nelson, N. (2019). Managing crop nutrients to achieve water quality goals. *Journal of Soil and Water Conservation*, *74*(5), 91A–101A. https://doi.org/10.2489/jswc.74.5.91a

Smith, V. H. (1982). The nitrogen and phosphorus dependence of algal biomass in lakes: An empirical and theoretical analysis 1. *Limnology & Oceanography*, *27*(6), 1101–1111. https://doi.org/10.4319/lo.1982.27.6.1101

Smith, V. H., & Schindler, D. W. (2009). Eutrophication science: Where do we go from here? *Trends in Ecology & Evolution*, *24*(4), 201–207. https://doi.org/10.1016/j.tree.2008.11.009

Snortheim, C. A., Hanson, P. C., McMahon, K. D., Read, J. S., Carey, C. C., & Dugan, H. A. (2017). Meteorological drivers of hypolimnetic anoxia in a eutrophic, north temperate lake. *Ecological Modelling*, *343*, 39–53. https://doi.org/10.1016/j.ecolmodel.2016.10.014

Søndergaard, M., Bjerring, R., & Jeppesen, E. (2013). Persistent internal phosphorus loading during summer in shallow eutrophic lakes. *Hydrobiologia*, *710*(1), 95–107. https://doi.org/10.1007/s10750-012-1091-3

Søndergaard, M., Jeppesen, E., Lauridsen, T. L., Skov, C., Van Nes, E. H., Roijackers, R., et al. (2007). Lake restoration: Successes, failures and long-term effects. *Journal of Applied Ecology*, *44*(6), 1095–1105. https://doi.org/10.1111/j.1365-2664.2007.01363.x

Staehr, P., Bade, D., Van de Bogert, M., Koch, G., Williamson, C., Hanson, P., et al. (2010). Lake metabolism and the diel oxygen technique: State of the science. *Limnology and Oceanography: Methods*, *8*(11), 628–644. https://doi.org/10.4319/lom.2010.8.0628

Steinsberger, T., Schwefel, R., Wüest, A., & Müller, B. (2020). Hypolimnetic oxygen depletion rates in deep lakes: Effects of trophic state and organic matter accumulation. *Limnology & Oceanography*, *65*(12), 3128–3138. https://doi.org/10.1002/lno.11578

Stone, M., & English, M. (1993). Geochemical composition, phosphorus speciation and mass transport of fine-grained sediment in two Lake Erie tributaries. *Hydrobiologia*, *253*(1–3), 17–29. https://doi.org/10.1007/bf00050719

Van Meter, K., Van Cappellen, P., & Basu, N. (2018). Legacy nitrogen may prevent achievement of water quality goals in the Gulf of Mexico. *Science*, *360*(6387), 427–430. https://doi.org/10.1126/science.aar4462

Van Meter, K. J., McLeod, M., Liu, J., Tenkouano, G. T., Hall, R., Van Cappellen, P., & Basu, N. (2021). Beyond the mass balance: Watershed phosphorus legacies and the evolution of the current water quality policy challenge. *Water Resources Research*, *57*(10), e2020WR029316. https://doi.org/10.1029/2020wr029316

21698961, 2023, 12, Downloaded from https://agupubs.onlinelibrary.wiley.com/doi/10.1029/2023JG007620, Wiley Online Library on [12/12/2023]. See the Terms and Conditions (https://onlinelibrary.wiley.com/terms-and-conditions) on Wiley Online Library for rules of use; OA articles are governed by the applicable Creative Commons License

Walsh, J. R., Corman, J. R., & Munoz, S. E. (2019). Coupled long-term limnological data and sedimentary records reveal new control on water quality in a eutrophic lake. *Limnology & Oceanography*, *64*(S1), S34–S48. https://doi.org/10.1002/lno.11083

Winslow, L. A., Zwart, J. A., Batt, R. D., Dugan, H. A., Woolway, R. I., Corman, J. R., et al. (2016). LakeMetabolizer: An R package for estimating lake metabolism from free-water oxygen using diverse statistical models. *Inland Waters*, *6*(4), 622–636. https://doi.org/10.1080/iw-6.4.883

Xia, Y., Mitchell, K., Ek, M., Sheffield, J., Cosgrove, B., Wood, E., et al. (2012). Continental-scale water and energy flux analysis and validation for the North American land data assimilation system project phase 2 (NLDAS-2): 1. Intercomparison and application of model products. *Journal of Geophysical Research*, *117*(D3), D03109. https://doi.org/10.1029/2011jd016048

References From the Supporting Information

Blais, J. M., & Kalff, J. (1995). The influence of lake morphometry on sediment focusing. *Limnology & Oceanography*, *40*(3), 582–588. https://doi.org/10.4319/lo.1995.40.3.0582

Carlson, R. E. (1977). A trophic state index for lakes 1. *Limnology & Oceanography*, *22*(2), 361–369. https://doi.org/10.4319/lo.1977.22.2.0361

Hanson, P. C., Pace, M. L., Carpenter, S. R., Cole, J. J., & Stanley, E. H. (2015). Integrating landscape carbon cycling: Research needs for resolving organic carbon budgets of lakes. *Ecosystems*, *18*(3), 363–375. https://doi.org/10.1007/s10021-014-9826-9

Hipsey, M. R., Bruce, L. C., Boon, C., Busch, B., Carey, C. C., Hamilton, D. P., et al. (2019). A general lake model (GLM 3.0) for linking with high-frequency sensor data from the global lake ecological observatory network (GLEON). *Geoscientific Model Development*, *12*(1), 473–523. https://doi.org/10.5194/gmd-12-473-2019

McCullough, I. M., Dugan, H. A., Farrell, K. J., Morales-Williams, A. M., Ouyang, Z., Roberts, D., et al. (2018). Dynamic modeling of organic carbon fates in lake ecosystems. *Ecological Modelling*, *386*, 71–82. https://doi.org/10.1016/j.ecolmodel.2018.08.009

Solomon, C., Bruesewitz, D., RichardsonRoseRose, D. C. K. C. K., Van de Bogert, M., Hanson, P., Kratz, T., et al. (2013). Ecosystem respiration: Drivers of daily variability and background respiration in lakes around the globe. *Limnology & Oceanography*, *58*(3), 849–866. https://doi.org/10.4319/lo.2013.58.3.0849

Wilkinson, G. M., Pace, M. L., & Cole, J. J. (2013). Terrestrial dominance of organic matter in north temperate lakes. *Global Biogeochemical Cycles*, *27*(1), 43–51. https://doi.org/10.1029/2012gb004453

21698961, 2023, 12, Downloaded from https://agupubs.onlinelibrary.wiley.com/doi/10.1029/2023JG007620, Wiley Online Library on [12/12/2023]. See the Terms and Conditions (https://onlinelibrary.wiley.com/terms-and-conditions) on Wiley Online Library for rules of use; OA articles are governed by the applicable Creative Commons License